The Journal of the Oceanological Society of Korea
Vol. 28, No. 4, pp. 292-304, December 1993

A Numerical Modeling of the East Sea Circulation

YOUNG HO SEUNG AND KYUN KIM
Dept. of Oceanography, Inha Univ., Inchon 402-751

동해 순환의 수치모델

승영호 · 김 균
인하대 해양학과

The East Sea circulation is numerically modeled with refined grid resolution elaborated open boundary condition, and by directly imposing the measured surface temperature and salinity. Typical features of the East Sea circulation are successfully modeled. The North Korean Cold Current and the East Korean Warm Current are clearer than those in previous works. Among others, the Ulleung Warm Water and the Intermediate Water of minimum salinity are nicely reproduced.

The latter is formed in the northern/northwestern coastal region in winter and is advected southward by strong under-current. The former is associated with a locally generated anti-cyclonic gyre. The model indicates strong seasonal variation of Nearshore Current along the Japanese coast, from wintertime barotropic to summertime baroclinic structures. The associated strong reversed under-current in summer is not well understood. Global circulation pattern is characterized by two regions of cyclonic and anti-cyclonic gyres in the north and south, respectively. The presence of these gyres indicates importance of local dynamics in East Sea circulation. This model, however, does not completely resolve the problem of overshooting of the East Korean Warm Current.

세밀한 격자망과 정교한 개방경계 조건을 적용하고 실측 수온 염분치를 직접 표층에 적용하여 동해순환을 수치 모델화 하였다. 동해의 특징적인 현상들이 성공적으로 재현되었으며 특히 북한한류와 동한난류가 더욱 뚜렷하여졌다. 특기할 만한 사실로는 울릉난수괴와 중층 저염분수가 재현되었다는 것이다. 전자는 동한난류의 바깥쪽에서 국지적으로 생성된 시계방향의 재순환류와 연관되어 있고 후자는 동해 북,북서 연안역에서 침강으로 형성되어 강한 중층해류에 의해 연안을 따라 남쪽으로 이동된다. 모델에서는 또한 일본 연안류가 강한 계절변화를 보여서 겨울에는 순압, 여름에는 경압구조를 나타냄을 보였으며 이 때 여름에 나타나는 강한 중층 반류가 흥미롭다. 모델에서는 또한 동해 순환의 거시적 특징을 지워 주는데 북쪽의 반시계 방향 순환역과 남쪽의 시계방향 순환역이 그것이다. 이들은 동해에서 국지적인 순환역학의 중요성을 시사한다. 그러나 본 모델에서는 동한난류의 이안점이 실제보다 북쪽에 치우쳐서 나타나는 것을 완전히 해결하지는 못하였다.

INTRODUCTION

The general feature of hydrography of the East Sea has been summarized by Moriyasu(1972): A very deep, cold and nearly homogeneous water, called the Japan Sea Proper Water, occupies the lower part of the basin. The upper thin layer is dynamically more active and can be divided into two regions, namely, the warm region in the south/southeast and the cold region in the north/northwest. In the former, the Tsushima Current (TC) Water dominates, which enters into the basin through the Korea Strait between Korea and Japan in the south, and flows out through the Soya and Tsugaru Straits in the northern part of Japan. In the latter, coastal waters of low salinity are typi-

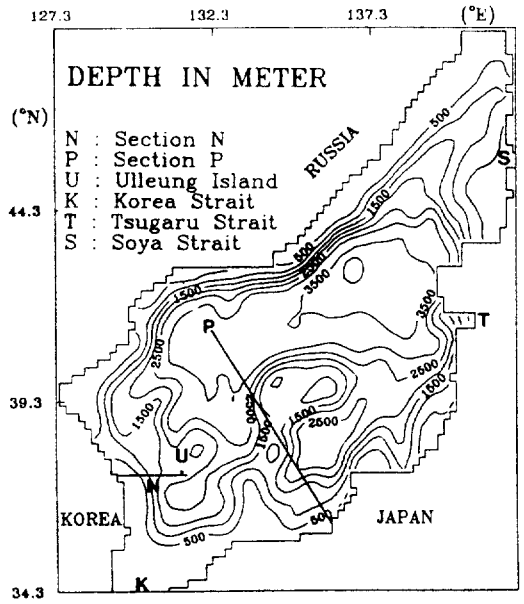

Fig. 1. Configuration of model domain and its topography.

cal off Siberia (Russia) and North Korea (c.f., Fig. 1).

Below the surface, the warm and saline TC Water is found in the warm region and high oxygen water is found in the cold region. The latter is also found in the warm region beneath the TC Water, forming the East Sea Intermediate Water (ESIW) of salinity minimum (Uda, 1934; Kim and Chung, 1984; Kim et al., 1991). This ESIW probably comes from the surface of the cold region. However, the detailed physical process about it is not yet known. The surface and subsurface hydrography described above is known to undergo a seasonal change, especially after cold winters (Hong et al., 1984; Kim & Legeckis, 1986; Seung and Nam, 1991).

The Volume transport of TC is believed to be about 1-2 Sverdrup and has large annual fluctuation (Yi, 1966). This current, after entering the basin, is known to split into 3 branches (Uda, 1934). The first one, called the Nearshore Branch (NB), flows along the Japanese coast. Yoon (1982c) explains that this branch is topographically controlled.

The third branch, called the East Korean Warm Current (EKWC), flows northward along the Korean coast and separates from the coast where it meets the southward flowing North Korean Cold Current (NKCC). The second branch, less clear, may exist along the slope near Japan. According to Kawabe (1982), it becomes prominent only in summer; it consists of disturbances generated at the inlet by increase of TC volume transport, topographically trapped and propagates along the slope. The EKWC and NKCC, after separation from the coast, form a strong front which runs in the east-west direction across the basin. Most of the EKWC flows out through outlets but the NKCC makes a cyclonic recirculation gyre in the north (Uda, 1934). Seung (1992) explains, using a simple model, the formation of NKCC and separation of EKWC as due to local forcings by wind and buoyancy flux. Along the front, large meanders develop associated with warm and cold eddies. In fact, there has been a different view about branching of the TC (Naganuma, 1973); it emphasizes the role of meandering rather than branching.

Apart from the global features noted above, some local observations are worth mentioning. One is the frequent observations of warm water accumulation off the Korean coast at about 37°N near the Ulleung Island (e.g. Kang and Kang, 1990; Kim, 1991); this water mass is called Ulleung Warm Water (UWW) hereafter. It is believed to be the center of a quasi-permanent anti-cyclonic gyre. Another is the presence of deep southward current measured directly (Lie et al., 1989) near Korean coast at about 800 m depth.

Numerical modelings of East Sea circulation have been initiated by Yoon (1982a, b and c). Each of these models shows one of three typical features: formations of the NB and EKWC and seasonal variation of circulation. However, any complete single model incorporating all these features has not been attempted yet. Recently, Kim (1991) has also tried to simulate the East Sea Circulation. However, many problems remain unsolved. All these models have been relatively coarse-gridded, and many of their results have not been rigorously compared with available observations. These models do not show, among others, the

Table 1. Level thickness of the model

level	1-2	3-4	5-12	13	14	15	16	17	18	19	20-23
thickness (m)	20	30	50	75	100	125	150	200	300	400	500

presences of the ESIW of salinity minimum and the UWW which are typical of southwestern part of the basin off the Korean coast. In these models, the EKWC and NKCC are successfully modeled, but the former overshoots the realistic separation position and the latter is not so persistent.

In this study, we present a numerical model which uses better grid resolution, in both horizontal and vertical directions, than before. To remove the uncertainties in surface fluxes of heat and water vapor, surface temperature and salinity based on available historical data are imposed directly as surface boundary condition. Open boundary condition for temperature and salinity is more elaborated by using either the radiation condition or prescribed values, depending on the advection condition. Baroclinic velocities at the inflow opening are also computed directly from the equations of motion. In the following second section, we describe about the setting of the model. In the third section, comparisons between model results and observations are made. Finally in the fourth section, discussions are made about model results before, in section 5, conclusions are drawn.

MODEL

The numerical model used here is by Cox (1984), which is a refinement of the model by Semtner (1974). As is commonly done in many OGCM, this model is based on the spherical coordinates and assumes rigid-lid surface. The model uses the B-grid configuration and the finite differencing is such that mass, heat, salt, variances of temperature, salinity and total energy are conserved in the model domain. Other detailed descriptions about the model are referred to Cox (1984).

The model domain (Fig. 1) is divided into horizontal grid of $0.2°\times0.2°$, in latitude and longitude. Vertically, it is consisted of 23 levels (Table. 1). In the initial state, it is assumed that there is no effect of the inflowing TC water and the whole basin is filled with the water of 0℃ and 34.1‰ which are close to the temperature and salinity of the Japan Sea Proper Water.

The surface temperature and salinity data used for surface boundary condition are those from Japan Oceanographic Data Center (e.g., 1978). Data are sufficient in areas covered by Korean and Japanese routine observations but largely insufficient elsewhere especially in the north/northwestern part of the basin. With these data, harmonic constants of annual and bi-annual components are found at each available data point. Spatial interpolation and extrapolation of harmonic constants are then made using the cubic spline method so that tracer (temperature and salinity) values are available at all grid points at any time.

Likewise, the same procedures are applied to the surface and open boundary conditions for momentum flux and tracers, respectively: wind stress at the surface (Na et al., 1992) and tracers over the vertical section of inflow opening (e.g., Fisheries Research and Development Agency, 1986) are harmonically analysed and the resulting harmonic constants are interpolated and extrapolated. However, in extrapolating the surface temperature to the area of insufficient data, i.e., northern/northwestern part of the basin, it was constrained to be higher than 0℃. This is to keep the surface water always lighter than the bottom water. In other words, it is assumed in this model that the winter convection occuring in the north/northwest of the basin does not penetrate deep to the bottom.

The measured tracer values are used in the surface boundary condition of the model as follows: Over the surface of the basin, a hypothetical level is assumed, which has the prescribed observed temperature and salinity. At the surface, a strong vertical diffusion is then allowed. The diffusion coefficient is taken as 100 cm^2/s which gives a dif-

fusive time scale of about 5.6 hours. This is quite negligible compared with the seasonal time scale considered here so that the response can be thought of as quasi-instantaneous. In the inflow open boundary condition of the model, the measured tracers are used in exactly the same way as that proposed by Stevens (1991). In this method, the tracers on the boundary are normally computed by using radiation boundary condition. If the velocity on the boundary is into the domain, then, the measured prescribed values are imposed. In the latter process, no relaxation time is needed in keeping computation stable. Baroclinic velocities on the open boundary are directly computed from the equation of motion as done by Stevens (1991). Since the outflow openings are much narrower than the inflow opening, simpler conditions are applied: gradient of tracers and baroclinic velocities are assumed vanishing along each outflow channel axis. This assumption does not raise any continuity problem because the depths are held unchanged along these axes. The same assumption is also made by Yoon (1982a, b) and Kim (1991). Differently from conditions for tracers and baroclinic velocities, stream functions (transports) are held fixed across the open boundaries. The total transport is taken as 1.6 Sverdrup. This is shared by the northern outlet (Soya Strait) and the southern outlet (Tsugaru Strait): 0.4 Sv for the former and 1.2 Sv for the latter.

Horizontal eddy coefficients are taken as 5.0×10^6 cm^2/s for viscosity and 1.0×10^6 cm^2/s for diffusivity. Vertical eddy coefficients are taken as 1.0 cm^2/s for viscosity and as 0.1 cm^2/s for diffusivity. The latter is one tenth smaller than the former. As suggested by Bryan (1987), this is to prevent the over-thickening of the TC water; the consequence of over-thickening is discussed later. Due to the surface cooling in winter, the water column becomes vertically unstable. This is overcome by allowing a very large vertical diffusion coefficient, 10^4 cm2/s here, which induces an immediate vertical mixing. This procedure is also taken when applying the surface boundary condition for tracers, as mentioned earlier. Since the model uses wide range of variable vertical diffusion coefficients, an implicit scheme is employed in calculating vertical diffusion processes.

COMPARISON WITH OBSERVATIONS

After about 60-years of run, the model results reached quasi-steady state: they show repeated annual variation without any significant long term trend. Tracers in the first level show similar distribution pattern as those observed (Fig. 2). In the fifth level (125 m), however, discrepancies are remarkable between the modeled and observed tracers (e.g., Fig. 3): In the model, the narrow southward intrusion of cold water along the western coast is not clear and, consequently, separation of the EKWC occurs farther north than expected. It seems that the model overestimates the inertial effect of western boundary current; it appears more enhanced in summer when the current becomes stronger (Fig. 4). More discussions about overshooting of the EKWC are given later.

At about 200 m depth, current becomes weaker and the similarity to the observation is again recovered as shown by the annual mean temperature distribution (Fig. 5). At this depth, the model shows the presence of warm water accumulation (temperature higher than 4.5℃ in Fig. 5) at the center of the anti-cyclonic gyre off the Korean coast. This might be a reproduction of the observed UWW (temperature higher than 3℃ in Fig. 5) indicating that the UWW is associated with a local anti-cyclonic gyre.

Model results are also compared well with the observed temperature and salinity section (called section P) across the basin, for example, with the one undertaken by Seifu Maru in 1964 (e.g., Fig. 6). This fact indicates that the model reproduces the basin-scale features satifactorily.

Another reference is the section (called section N) along 37.33°N off the Korean coast accross the EKWC, for example the one undertaken by KORDI in 1984 (Fig. 7). The warm and saline core of the EKWC , at about 129.3°E, is nicely reproduced by the model and the presence of the UWW, at about 130.1°E, can be remarked too. Most of all, the reproduction of the ESIW of sali-

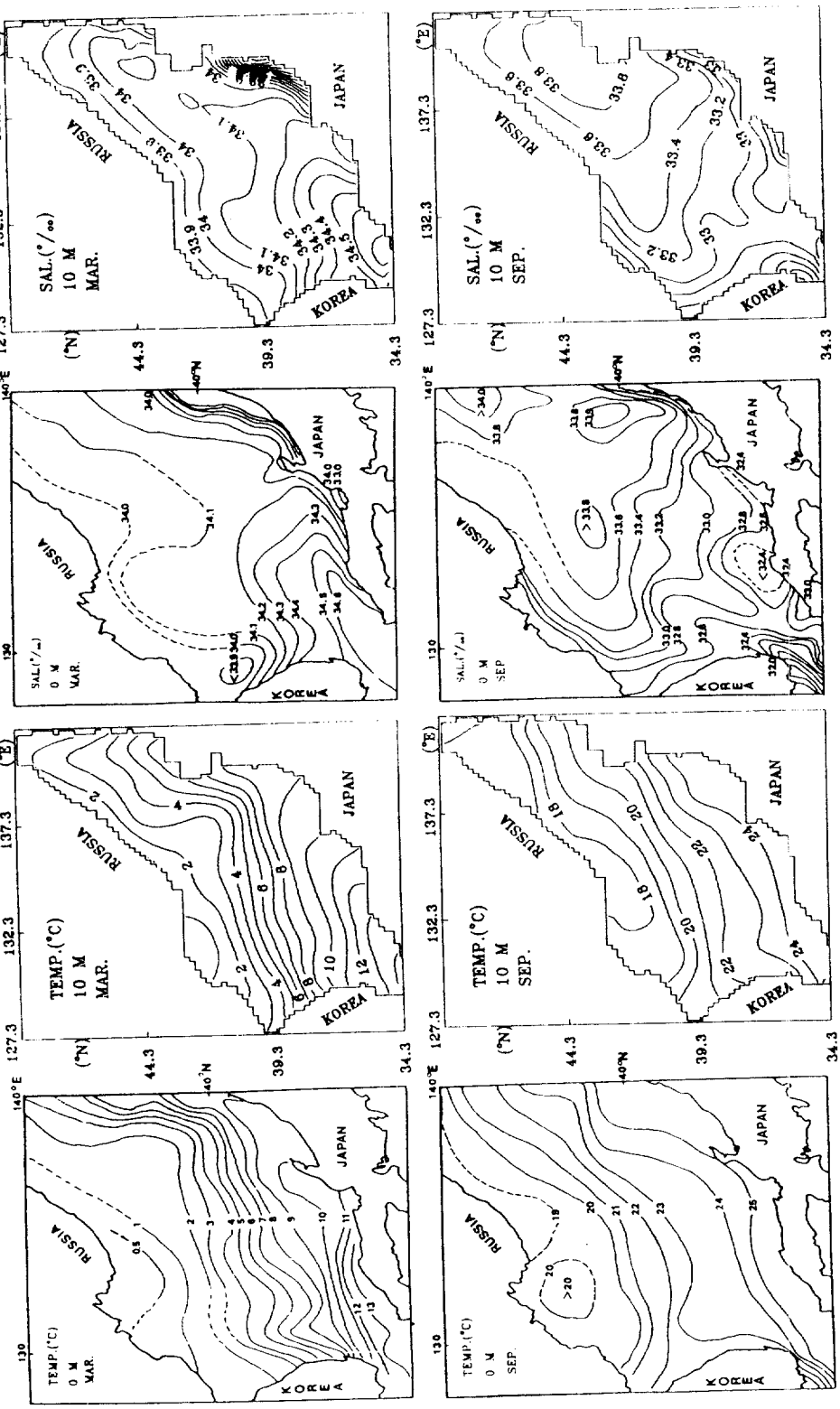

Fig. 2. Horizontal distributions of temperature (left half) and salinity (right half) in March (upper) and September (lower) obtained from observation (0 m depth) and model experiment(10 m depth).

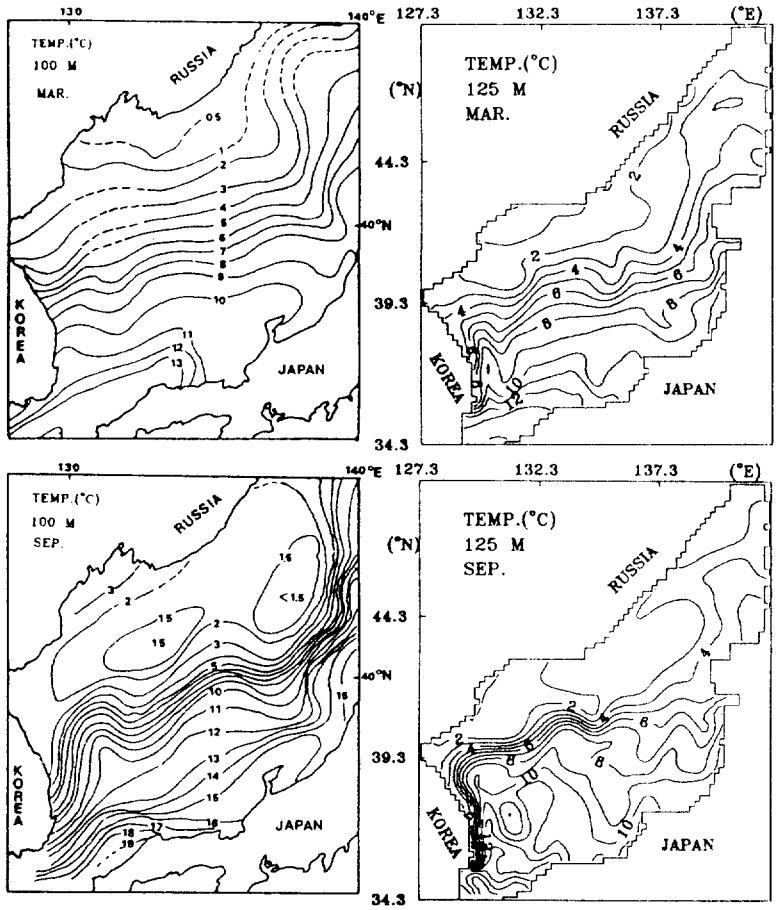

Fig. 3. Horizontal distributions of temperature in March (upper) and September (lower) obtained from observation (100 m depth) and model experiment (125 m depth).

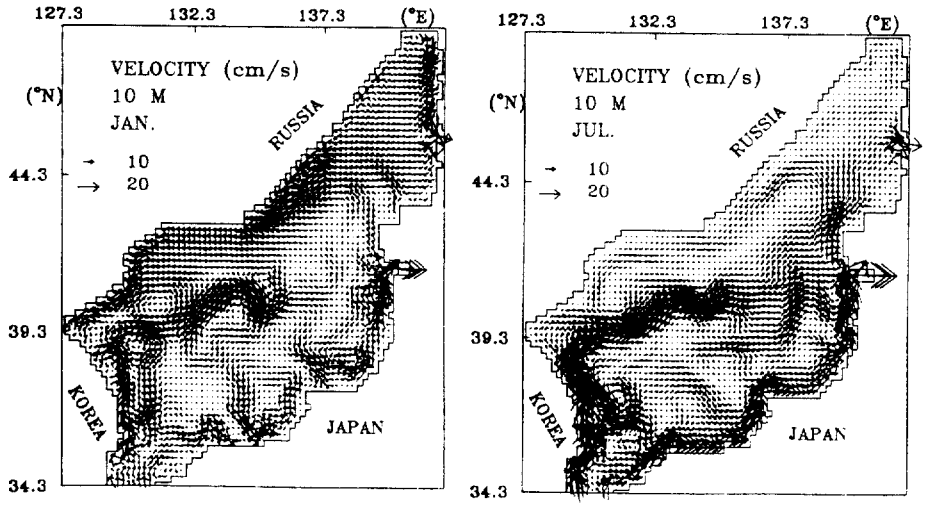

Fig. 4. Current velocity fields at 10 m depth (first level) in January and July.

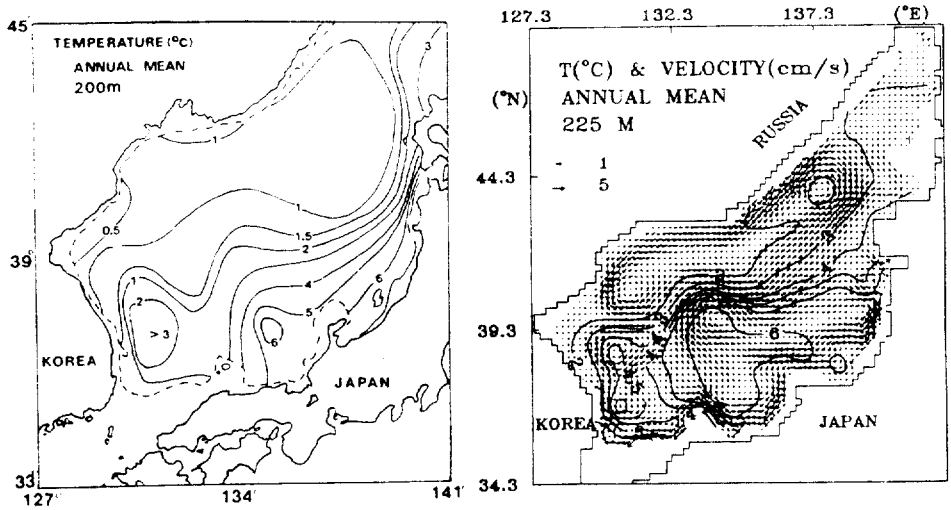

Fig. 5. Distributions of annual mean temperature observed(200 m depth) and model-computed(225 m depth). The former is compiled by JODC (1975). For comparison, model-computed current vectors are overlaid.

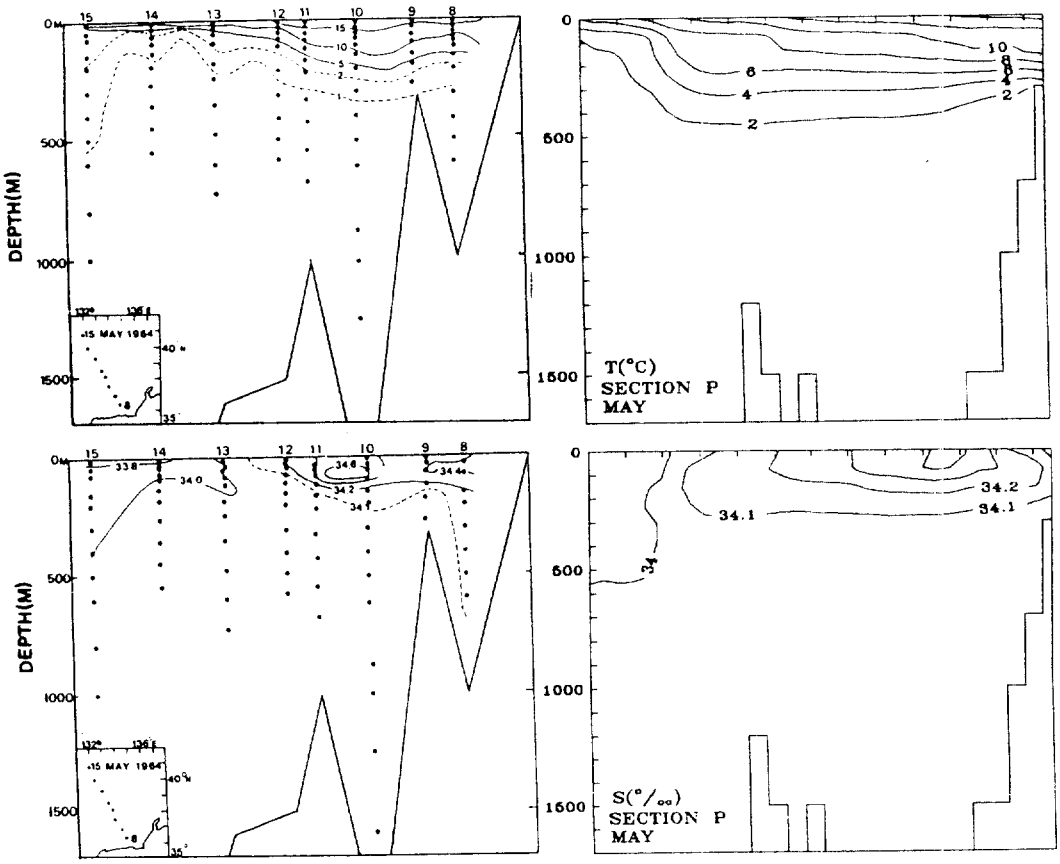

Fig. 6. Vertical sections of temperature (upper) and salinity (lower) across the basin (section P, see Fig. 1) observed in 1964 by Seifu Maru (left) and obtained from model experiment (right), both in May.

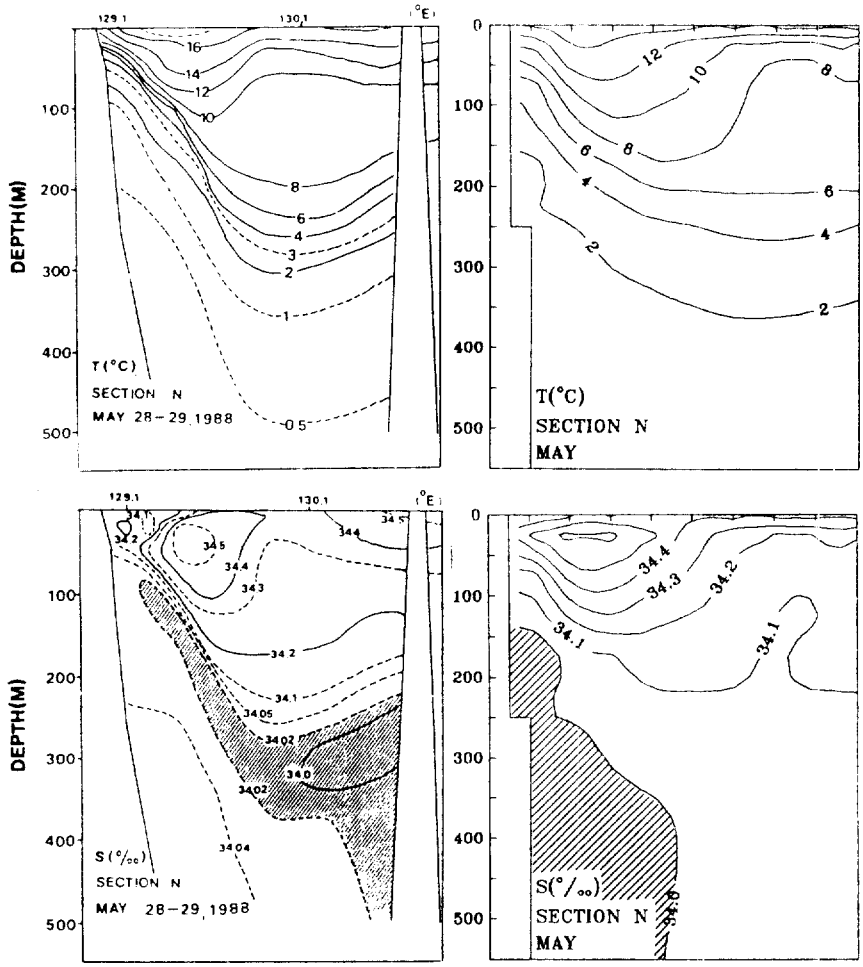

Fig. 7. Vertical sections of temperature (upper) and salinity (lower) along the latitute 37.330 N off Korean coast (section N, see Fig. 1) observed in 1988 by KORDI (left) and obtained from model experiment (right), both in May.

nity minimum is quite encouraging. In the model, it is thicker and appears closer to the side boundary than that in observation. Other observations (c.f., Kim et al., 1991) indicate that the location and shape of the ESIW vary from year to year so that the direct comparison between a particular observation and the model result shown in Fig. 7 can be hardly the same. On a larger scale (extension of the section N along the same latitude, see Fig. 8), the layer of salinity minimum extends over large area of the basin. More discussions about the ESIW are given in the next section. It should be noted, however, that, in the model (Fig. 7), there is no fresh water just off the coast, probably due to the overshooting of the EKWC.

The current at 875 m depth off the Korean coast undergoes a seasonal fluctuation even though the current is very weak. It is northward in winter but becomes southward in summer season (Fig. 9) confirming the measurements (Lie et al., 1989).

DISCUSSION

Despite some deficiencies, the separation of the EKWC and formation of the persistent NKCC are clear (Fig. 4). The major surface currents are the EKWC, NKCC and NB, but the so called the second branch is not clear. The NKCC extends

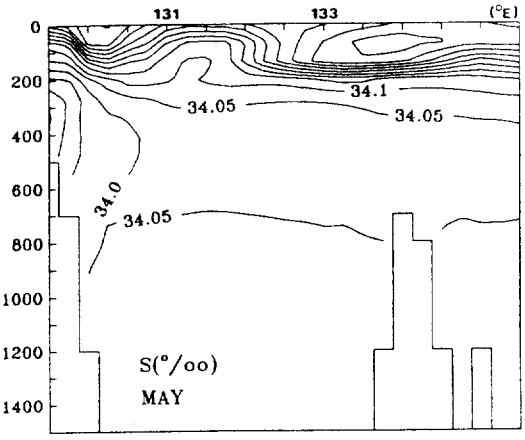

Fig. 8. Vertical section of salinity along the extended line of section N in May.

southward down to about 40°N in summer, and moves further south to about 39°N in winter. However, it is generally believed that the NKCC extends more to the south. A part of the EKWC, after separation, flows offshore making large meanders and the rest of it deviates southward making a recirculation of the EKWC and local anti-cyclonic gyres in it. One of these gyres forms the UWW at its center. More discussions about the generation of these gyres will be given later.

Overshooting of western boundary current has long been a common problem in numerical modeling. Ezer and Mellor (1992) point out, in a series of numerical experiments on local Gulf Stream problem, that thermodynamic effect is fundamental in maintaining southward advection of cold water and thus preventing the overshooting of the Gulf Stream. In this respect, the incorrect surface boundary conditions of temperature and salinity in the north/northwest of the basin may be the major factor of the overshooting.

Bryan (1987) stresses the importance of the vertical diffusion coefficient in controlling both the thermocline depth and the overshooting. In our study, it is certain that the small vertical diffusion coefficient taken here has contributed to preventing the TC water from thickening but this does not seem to be the case for overshooting of the EKWC. Furthermore, it is not known whether there are any other factors involved, such as the isopycnal diffusivity of the horizontal mixing.

At the surface, both the EKWC and NB strengthen in summer but the NKCC strengthens in winter (Fig. 4). The formers seem to be due to the summer time intense baroclinic effect and the latter, due to the strong northerly monsoon winds prevailing in winter in this region. These winds may not only generate strong southward coastal currents but, due to the presence of strong negative wind stress curl in this part of the basin (Na et

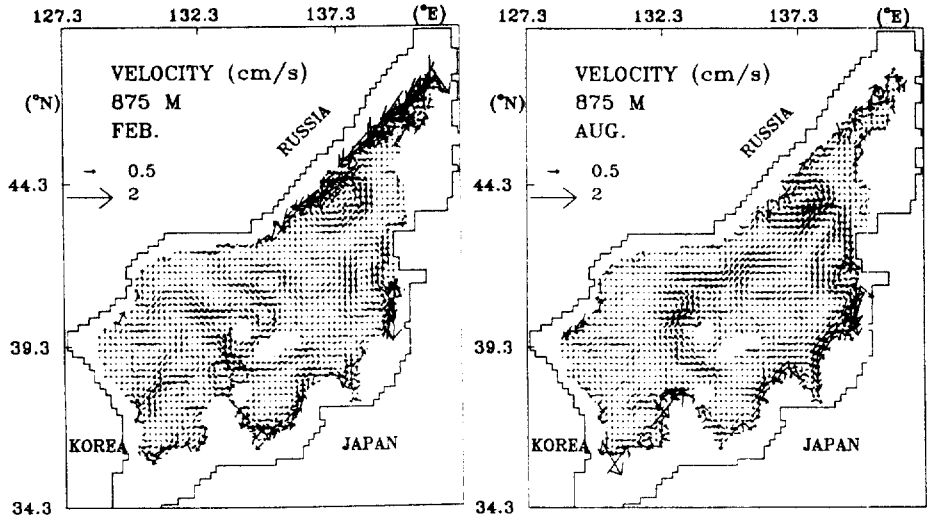

Fig. 9. Velocity fields at 875 m depth in February and August.

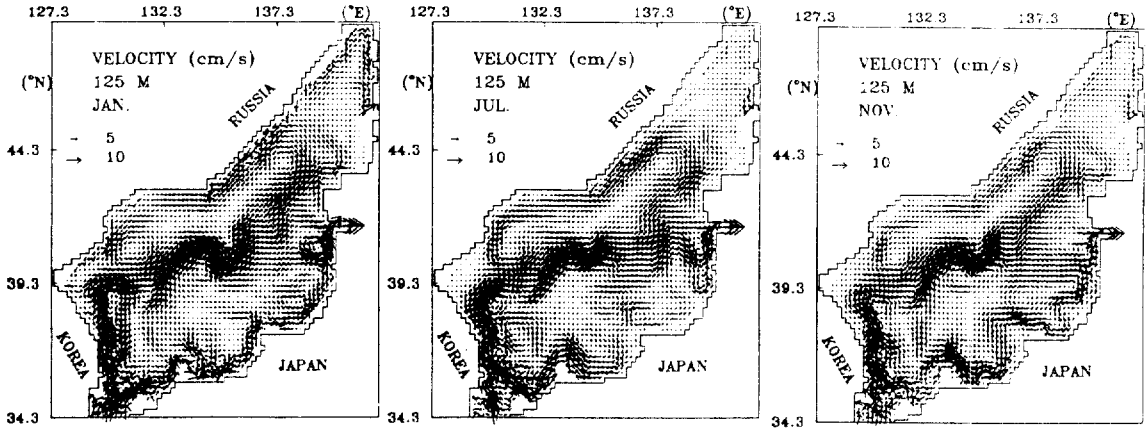

Fig. 10. Velocity fields at 125 m depth in January and July. That in November is presented to show the time evolution of velocity field.

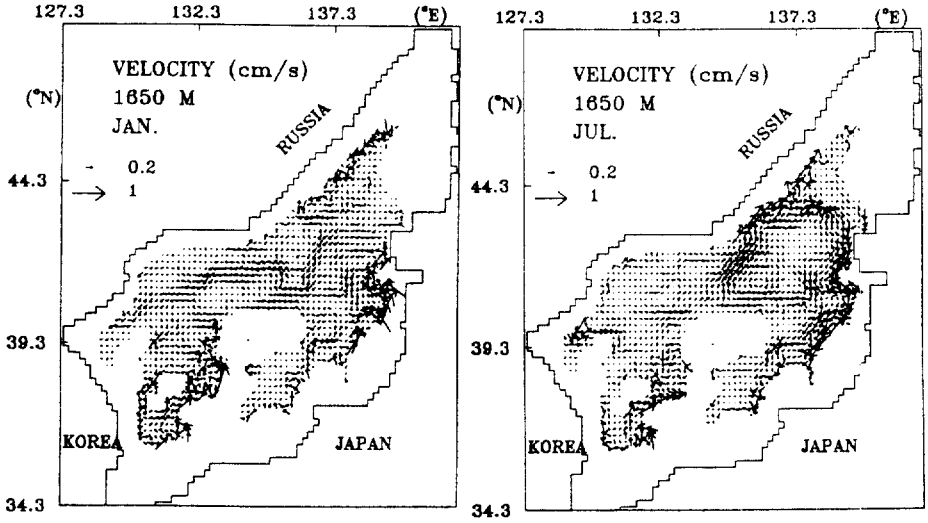

Fig. 11. Velocity fields at 1650 m depth in January and July.

at., 1992), also intensify the large-scale cyclonic gyre and therefore strengthen the southward alongshore current. Especially, the NB undergoes a large seasonal variation: it is largely barotropic in winter but occupies only the upper 100 m depth in summer by leaving the deeper parts to a strong under-current (Fig. 10). It is not yet understood how this under-current can be generated. The following explanation may be suggested: The imposed thermal front at the surface as a boundary condition in summer season generates baroclinic motions (disturbances) through continuous geostrophic adjustments. The baroclinic current fields thus generated along the front propagate westward, probably as Rossby waves, and then anti-clockwisely around the slope of the basin, probably as internal Kelvin waves. The progressive extension of this current field anti-clockwisely around the basin during the summer season until November (Fig. 10) seems to support this explanation.

Finally, It should be remarked that currents in deep layer undergo large seasonal variation (e.g., Fig. 11). This seems to be the effect of barotropic response to seasonally fluctuating wind in this ba-

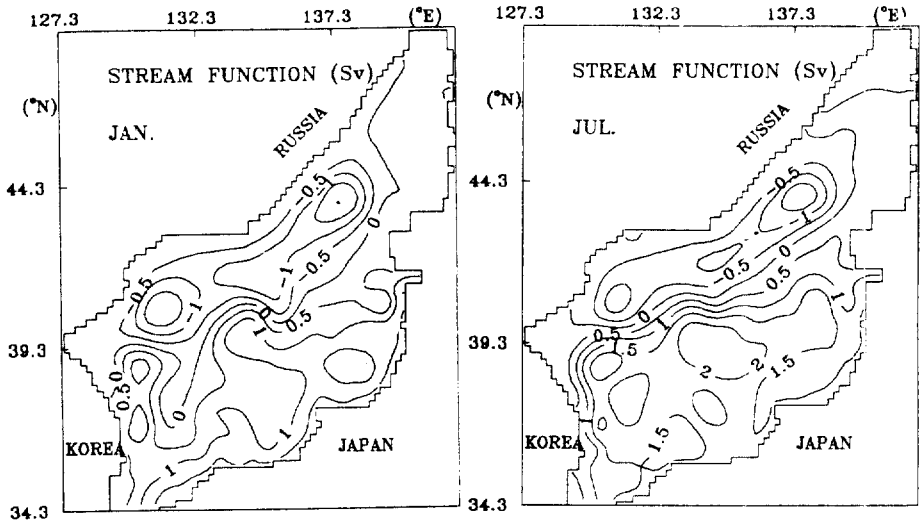

Fig. 12. Distributions of stream function in January and July.

sin.

The volume transport of each current undergoes a seasonal fluctuation. In summer, most of the transport through the inlet takes place by the EKWC and in winter, the volume transport of the NB becomes the greatest (Fig. 12). The transport of NB, which is the most barotropic in winter, seems to be most enhanced by topographic guide. The pattern of basin-scale stream function is characterized by two regions of cyclonic and anti-cyclonic gyres in the north and south, respectively (Fig. 12). These two regions are separated by the main stream of the TC which also coincides with the polar front(c.f., Fig. 3). In the northern half of the basin, there is a large cyclonic gyre which embraces two small cyclonic gyres at both sides, confirming the traditional view (e.g., Uda, 1934). In the southern half, there are several small anti-cyclonic gyres of which the one associated with the UWW is an example. It seems that the northern half is dominated by positive vorticity and the southern half, by negative vorticity.

The former might be due to strong positive wind stress curl (e.g., Na et al., 1992) and the latter may be associated with diffusion of negative vorticity created along the western boundary. In fact, the former strengthens in winter when strong wind of positive stress curl prevails in the north and the latter becomes more pronounced in summer when the EKWC is the strongest. These gyres are locally generated and their presence indicates the importance of local effects in the East Sea circulation.

One of major interesting features in the East Sea is the presence of the ESIW of salinity minimum. In this model, regions of fresh water source in winter (salinity lower than 34.0‰ in March in Fig. 2) are found along the northern/northwestern and the southeastern coasts. Since winter convection occurs only in the former, the ESIW must be formed in this area by sinking of surface water. This water may then be transported southward by current. In fact, the horizontal distribution of salinity at intermediate depth (425 m), in May for example, and the current field affecting the distribution, that in February for example, strongly support this hypothesis (Fig. 13). This current field does not change drastically through the year but the southward current contributing to the transport becomes the strongest in winter probably due to the combined effect of strong wind and wintertime barotropy. This model suggests us, therefore, that the southwestern part of the basin (off the Korean coast) is the area directly affected by young fresh water.

In another experiment without any restriction

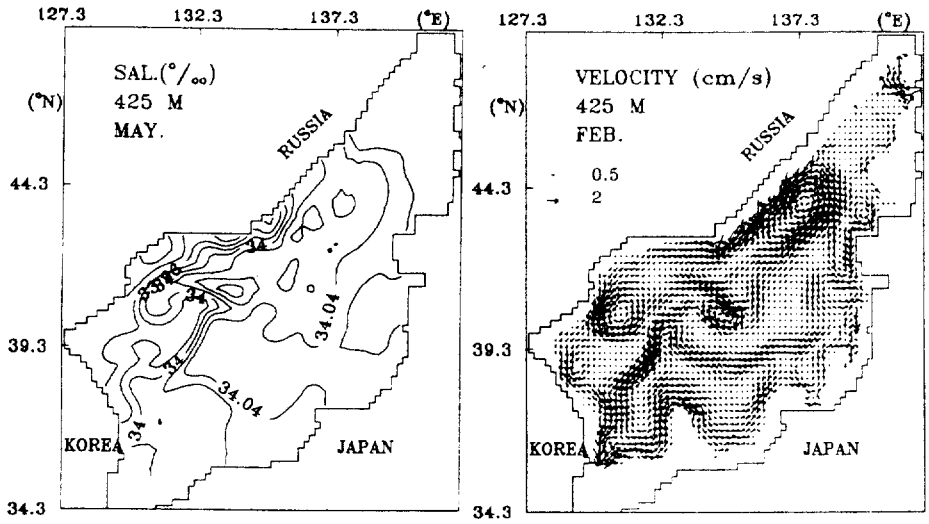

Fig. 13. Distribution of salinity in May and current field in February at 425 m depth.

on surface temperature condition, i.e., allowing deep winter convection, the formation of the fresh water extends to much deeper layers. On the other hand, employing larger value (1.0 cm^2/s) of vertical diffusion coefficient makes the TC Water much thicker extending from the surface down to the level beyond intermediate layer. The presence of thick TC Water largely prevents the southward movement of cold fresh water on the horizontal plane of intermediate depth. Result is the appearance of salinity minimum layer at much deeper layer. In this experiment, we realize therefore how the intermediate/deep layers are sensitive to surface boundary condition and vertical diffusion coefficient.

CONCLUSIONS

Progress in numerical modeling of the East Sea Circulation is made by increasing the grid resolution, elaborating the open boundary condition, eliminating, to some extent, the uncertainty of surface heat and salt fluxes by directly imposing the measured temperature and salinity on the surface, and by employing appropriate vertical diffusion coefficient.

Many observed features are successfully reproduced here: the general hydrography across the basin, branching of the TC into the EKWC and NB, separation of the EKWC, persistency of the NKCC and the presence of UWW; the UWW is associated with a local anti-cyclonic gyre.

Among others, the reproduction of the ESIW of salinity minimum, quite typical off the Korean coast, is encouraging. This water seems to be formed in the north/northwest by winter convection and advected southward along the coast by strong under-current. The advection seems to be the strongest in winter probably because of the combined effect of strong wind and barotropy.

Model results indicate strong seasonal change of current structure in the NB; from barotropic in winter to baroclinic in summer. In summer, the strong under-current of reversed direction is noteworthy. The model also characterizes the global circulation as two regions of cyclonic and anti-cyclonic gyres in the north and south, respectively. The former seems to be due to the positive wind stress curl, the strongest in winter, and the latter, due to the negative vorticity diffused from the EKWC which is the strongest in summer.

Despite some successes of the model, the overshooting of the EKWC still remains as the problem to be solved. There are many other numerical results that await proper explanations. Among others, the formaton of the anti-cyclonic gyre asso-

ciated with the UWW may be explained by applying the vorticity dynamics and might be a good subject of next work. The generation of the southward under-current along the Japanese coast should first be confirmed by observation before any attempt of dynamic explanation is made.

ACKNOWLEDGEMENTS

This study is an output of 1990-1993 KOSEF research support program. Discussions with Dr. J.H. Yoon at RIAM/Kyushu University, Japan were useful.

REFERENCES

Bryan, F., 1987. Parameter sensitivity of primitive equation ocean general circulation models. *J. Phys. Oceanogr.*, **17**: 970-985.

Cox, M.D., 1984. A primitive equation, 3-dimensional model of the ocean.GFDL Ocean Group Technical Report No.1, GFDL/NOAA, Princeton Univ.

Ezer, T. and G.L. Mellor, 1992. A numerical study of the variability and the separation of the Gulf Stream, induced by surface atmospheric forcing and lateral boundary fows. *J. Phys. Oceanogr.*, **22**: 660-682.

Korea Fisheries Research and Development Agency, 1986. Mean oceanographic charts of the adjacent seas of Korea. Pusan, Korea., 186pp.

Hidaka, K. and T. Suzuki, 1950. Secular variation of the Tsushima Current. *J. Oceanogr. Soc. Japan*, **16**: 28-31.

Hong, C.H., K.D. Cho and S.K. Yang, 1984. On the abnormal cooling phenomenon in the coastal areas of East Sea of Korea in Summer 1981. *J. Oceanol. Soc. Korea*, **19**: 11-17.

Japan Oceanographic Data Center, 1975. Marine Environmental Atlas, Northwestern Pacific Ocean: Statistics of the Oceanographic Elements (all months)Japan Hydrographic Association.

Japan Oceanographic Data Center, 1978. Marine Environmental Atlas, Northwestern Pacific Ocean I: Seasonal and Monthly. Japan Hydrographic Association.

Kang, H.E. and Y.Q. Kang, 1990. Spatio-Temporal characteristics of the Ullung Warm Lens. Bull. Korean Fish. Soc. **23**: 407-415.

Kawabe, M., 1982. Branching of the Tsushima Current in the Japan Sea. Part I: Numerical experiment. *J. Oceanogr. Soc. Japan*, **38**: 183-192.

Kim, C.H., H.J. Lie and K.S. Chu, 1991. On the Intermediate Water in the southwestern East Sea (Sea of Japan). "Oceanography of Asian Marginal Seas", K. Takano ed., Elsevier, 129-141.

Kim, H.R., 1991. The vertical structure and temperature variation of the intermediate homogeneous water near Ulleung Island. MSc thesis Seoul Nat. Univ. 84pp.

Kim, Y.E., 1991. A numerical study on the circulation of the East Sea (Japan Sea). PhD thesis, Seoul National Univ., 211pp.

Kim, K. and J.Y. Chung, 1984. On the salinity minimum and dissolved oxygen maximum layer in East Sea. "Ocean hydrodynamics of the Japan and East China Sea", T.Ichiye ed., Elsevier, Amsterdam, 55-65.

Kim, K. and R. Legeckis, 1986. Branching of the Tsushima Current in 1981-83. Progr. Oceanogr., **17**: 265-276.

Lie, H.J., M.S. Suk and C.H. Kim, 1989. Observations of southeastward deep currents off the east coast of Korea. *J. Oceanol. Soc. Korea*, **24**: 63-68.

Moriyasu, S., 1972. The Tsushima Current. In "Kuroshio", H.Stommel and K. Yoshida ed., Univ. of Washington Press, 353-369.

Na, J.Y., J.W. Seo and S.K. Han, 1992. Monthly-mean seasurface winds over the adjacent seas of the Korean Peninsula. *J. Oceanol. Soc. Korea*, **27**: 1-10.

Naganuma, K., 1973. A discussion on the existence of Tsushima Current third sub-branch. News Fish. *Res. Japan Sea*, No.266.

Semtner, A.J., 1974. An oceanic general circulation model with bottom topography. UCLA Dept. of Meteorol. *Tech. Rep.* No.9, 99pp.

Seung, Y.H. and S.Y. Nam, 1991. Effects of winter cooling on subsurface hydrographic conditions off Korean coast in the East (Japan) Sea.

"Oceanography of Asian Marginal Seas", K. Takano ed., Elsevier, 163-178.

——, 1992. A simple model for separation of East Korean Warm Current and formation of North Korean Cold Current. *J. Oceanol. Soc. Korea*, **27**: 189-196.

Stevens, D.P., 1991. The open boundary condition in the United Kingdom fine-resolution Antarctic model. *J. Phys. Oceanogr.*, **21**: 1494-1499.

Uda, M., 1934. The results of simultaneous oceanographical investigations in the Japan Sea and its adjacent waters in May and June, 1932. *J. Imp. Fish. Exp. Sta.*, **5**: 57-190 (in Japanese).

Yi, S.U., 1966. Seasonal and secular variations of the water volume transport across the Korea Strait. *J. Oceanol. Soc. Korea*, **1**: 7-13.

Yoon, J.H., 1982a. Numerical experiment on the circulation in the Japan Sea, Part II: Formation of the East Korea Warm Current. *J. Oceanogr. Soc. Japan*, **38**: 43-51.

——, 1982b. Numerical experiment on the circulation in the Japan Sea. Part I: Influence of seasonal variations in atmospheric conditions on the Tsushima Current. J. Oceanogr. Soc. Japan **38**: 81-94.

——, 1982c. Numerical experiment on the circulation in the Japan Sea, Part III: Formation of the nearshore branch of the Tsushima Current. *J. Oceanogr. Soc. Japan*, **38**: 119-124.

Accepted November 2, 1993